Role of pumping statistics in micromasers

E. S. Guerra, A. Z. Khoury, L. Davidovich, and N. Zagury
Departamento de Física, Pontifícia Universidade Católica do Rio de Janeiro, Caixa Postal 38071, 22452 Rio de Janeiro, Rio de Janeiro, Brazil
(Received 23 April 1991)

We show that regularization of pumping leads to large photon-number noise reduction in one- and two-photon micromasers, and is much more important than in macroscopic lasers and masers. Our calculations are based on a step-by-step microscopic approach and are compared to results obtained from a pumping-statistics-dependent master equation, which is shown not to be entirely reliable in the micromaser case. Although noise reduction and the discrepancies betwen the two approaches are more important for monokinetic beams, they are still relevant when a 10% velocity dispersion is allowed.

PACS number(s): 42.50.Bs, 42.50.Dv, 42.52.+x

I. INTRODUCTION

Recent developments in cavity quantum electrodynamics have provided new tools for the investigation of the interaction of matter and radiation. Thus, the injection of beams of Rydberg atoms into superconducting cavities has rendered possible the realization of new kinds of masers, operating at very low thresholds, down to at most one atom at a time inside the cavity [1,2]. These devices have been called *micromasers,* and have allowed the testing of very basic models in quantum optics, displaying a variety of interesting phenomena, closely related to the quantum nature of the radiation field.

In particular, the field statistics in micromasers may be quite different from that of macroscopic lasers and masers [3,4]. Indeed, the field produced in these devices has been predicted [3,4] to be sub-Poissonian for a wide range of parameters and this has been experimentally confirmed [5]. For other parameters, the field may be strongly super-Poissonian and the photon distribution may have two or more peaks [3,4], thus characterizing a multistable behavior of the system.

In the experiments made so far, the incoming beam of excited atoms obeys with a very good approximation a Poissonian distribution with respect to the arrival times. On the other hand, it has been recently put into evidence that the statistics of the pumping may play an important role in the behavior of lasers and masers [6–8]. By injecting the atoms in a regular way, instead of the usual Poissonian distribution, one may obtain a substantial noise reduction in these devices. One might expect that even more important quieting should result in micromasers, due to their microscopic nature, and the stepwise atom-by-atom excitation of the field. If this is true, one would be able, by regularizing the incoming atomic flux, to get even narrower field distributions in these devices.

In the present paper we analyze the role of pumping statistics in one- and two-photon micromasers, and show that it is indeed possible to further reduce the variance of the field generated by these devices. In fact, due to their highly nonlinear nature, a reduction of the pumping noise may sometimes produce an increase of the photon-number uncertainty, which results from the appearance of multiple peaks of comparable magnitude in the photon-number distribution, as the pumping statistics is changed.

Other discussions presented so far in the literature on the micromaser case [7,9] have been based on a pumping-statistics-dependent master equation [7]. This approach makes a continuous approximation of the stepwise excitation mechanism, and requires therefore that the number of atoms and photons involved is sufficiently high (it could be termed in this sense *a mesoscopic* approach). Although this is certainly justified for usual (macroscopic) lasers and masers, this is not necessarily true for micromasers, where one deals frequently with a few atoms and photons.

This fact has prompted us to make a comparison between the microscopic atom-by-atom numerical solution and the mesoscopic master equation approach, thus checking its validity in this case [10]. We show that large discrepancies may indeed occur even if we allow a velocity dispersion in the atomic beam. They are more important precisely in the regions where the system is more sensitive to pumping statistics.

We start our work with a detailed analysis, in Sec. II, of the approximations involved in the derivation of the pumping-statistics-dependent master equation, as done by Bergou *et al.* [7], and extend this treatment to two-photon degenerate lasers and masers. In Sec. III we present the microscopic model for micromasers with Poissonian or regular pumping, obtaining recursion relations for the populations in both cases. In Sec. IV we discuss the numerical results, obtained from the stepwise microscopic approach, and check the validity of the corresponding calculations based on the master equation. In Sec. V we summarize our conclusions.

II. THE MASTER EQUATION APPROACH

Lasers and masers may be modeled [11] by a flux of atoms being injected into a cavity resonant with a transition $a \rightarrow b$ between two atomic levels. The atoms start interacting with the cavity in the excited state $|a\rangle$, the dis-

tribution of injection times defining the pumping statistics.

We assume that the cavity damping time is much larger than the interaction time between each atom and the cavity, which allows one to neglect the losses when considering any individual atomic evolution. The cumulative effect of the losses is then added *a posteriori*, through the usual reservoir terms in the master equation [11]. Although frequently adopted in laser theory, the separate treatment of the losses is not generally justifiable for micromasers. This point will be further examined at the end of this section.

Let us consider then an atom arriving at the cavity at time t_i. The change in the reduced field density operator ρ, due to the passage of the ith atom, may be written as

$$\rho(t_{i+1})=M\rho(t_i) , \tag{2.1}$$

where M is a superoperator which depends on the atom-field dynamics and on the initial conditions for each atom.

We will be interested mainly in the populations, $\pi_N=\rho_{NN}$, in the Fock (photon-number) representation. From Eq. (2.1), and considering that the atom arrives in the cavity in the excited state, we get [3,4] (we adopt the convention that $\pi_N=0$ whenever $N<0$)

$$\pi_N(t_{i+1})=(1-\beta_{N+\zeta})\pi_N(t_i)+\beta_N\pi_{N-\zeta}(t_i) , \tag{2.2}$$

where $\zeta=1$ (2) for the one-photon (two-photon degenerate) micromaser, while

$$\beta_{N+1}=\sin^2\Omega_{ab}\sqrt{N+1}t_{\rm int} \tag{2.3}$$

for the one-photon micromaser, and

$$\beta_{N+2}=\frac{4(N+2)(N+1)}{(2N+3)^2}\sin^2\frac{(2N+3)\Omega_{ac}^2}{2\Delta}t_{\rm int} \tag{2.4}$$

for the two-photon degenerate micromaser. In Eq. (2.4), Ω_{ac} is the one-photon Rabi frequency for the transition between the initial excited state $|a\rangle$ and an intermediate state $|c\rangle$ nearly halfway between the initial and the final states, with a detuning Δ with respect to that halfway point. The cavity is tuned to a frequency $\omega=(E_a-E_c)/\hbar$, and Δ is chosen so as to enhance the two-photon transition probability, while at the same time keeping negligible the resonant one-photon cascade $|a\rangle\rightarrow|c\rangle\rightarrow|b\rangle$. We have assumed for simplicity that $|\Omega_{ac}|=|\Omega_{cb}|$, where Ω_{cb} is the one-photon Rabi frequency between states $|c\rangle$ and $|b\rangle$. This condition is actually verified, with very good approximation, in the experiments made so far [2].

Bergou *et al.* [7] have shown that, if for the sake of concreteness one imagines a regular flux of atoms going at a rate R through an excitation region, right before entering the cavity, and if p is the probability that each atom be excited in that region from the atomic ground state to the lasing excited state $|a\rangle$, then the total change in the field reduced density operator, from an arbitrary time $t=0$ to a final time t, is

$$\rho(t)=[1+p(M-1)]^{Rt}\rho(0) , \tag{2.5}$$

where the excited atoms are supposed to contribute independently (no cooperative effects). As the parameter p varies from 1 to 0, one goes continuously from the regular pumping ($p=1$) case to the Poissonian pumping regime ($p\rightarrow 0$; $R\rightarrow\infty$; $r=pR$ finite).

If the number of injected atoms $K=Rt$ is large enough so that it may be treated as a continuous variable, we may write, as in Ref. [7], for the coarse-grained derivative of $\rho(t)$:

$$\frac{\Delta\rho}{\Delta t}\approx\frac{r}{p}\ln[1+p(M-1)]\rho(t) , \tag{2.6}$$

where

$$R\Delta t\gg 1 , \tag{2.7}$$

so that several atoms cross the cavity during Δt, and $r=Rp$ is the average rate of excited atoms entering the cavity. This approximation is valid as long as

$$R\Delta t|\ln[1+p(M-1)]|\ll 1 , \tag{2.8}$$

which is the condition for $\rho(t)$ not to change much during the time interval Δt. Since (2.7) must also hold, we see therefore that Eq. (2.8) is valid only for $|p(M-1)|\ll 1$ and we may thus expand Eq. (2.6) as

$$\frac{\Delta\rho}{\Delta t}\approx\dot\rho\approx r[(M-1)-\tfrac{1}{2}p(M-1)^2]\rho(t) . \tag{2.9}$$

As shown in Ref. [7], higher-order terms in this expansion do not contribute to the diffusion coefficient.

Losses are added to the rate equation in the usual way [11]:

$$L\rho=\frac{\omega}{2Q}(N_T+1)(2a\rho a^\dagger-a^\dagger a\rho-\rho a^\dagger a)+\frac{\omega}{2Q}N_T(2a^\dagger\rho a-aa^\dagger\rho-\rho aa^\dagger) , \tag{2.10}$$

where $a^\dagger(a)$ is the creation (annihilation) operator for a photon with frequency ω, Q is the quality factor of the cavity, and N_T is the mean photon number for a cavity in equilibrium at temperature T. From now on we set $N_T=0$ for simplicity. Using Eqs. (2.2), (2.9), and (2.10), we get the population rate equation for the micromaser:

$$\dot\pi_N=r(-\beta_{N+\zeta}\pi_N+\beta_N\pi_{N-\zeta})+\frac{rp}{2}[-\beta_{N+\zeta}^2\pi_N+(\beta_N^2+\beta_N\beta_{N+\zeta})\pi_{N-\zeta}-\beta_N\beta_{N-\zeta}\pi_{N-2\zeta}]+\frac{1}{t_{\rm cav}}[(N+1)\pi_{N+1}-N\pi_N] , \tag{2.11}$$

where $\zeta=1$ (2), $t_{\rm cav}=Q/\omega$, and the gain coefficients $\beta_{N+\zeta}$ are given by Eq. (2.3) [Eq. (2.4)] for the one- (two-) photon maser. For $p\rightarrow 0$,

$$\dot\pi_N=r(-\beta_{N+\zeta}\pi_N+\beta_N\pi_{N-\zeta})+\frac{1}{t_{\rm cav}}[(N+1)\pi_{N+1}-N\pi_N] , \tag{2.12}$$

which is the Scully-Lamb equation [10,11] for Poissonian

pumping.

Starting from Eq. (2.11), we can derive, as done in Ref. [7], the rate equations for the mean photon number and variance:

$$\begin{aligned}\langle \dot{N}\rangle &= \zeta r\langle \alpha_N\rangle - \gamma\langle N\rangle ,\\ \langle \dot{\Sigma}\rangle &= 2r\zeta\langle \alpha_N \Delta N\rangle + r\zeta^2\langle \alpha_N - p\beta_{N+\zeta}\beta_{N+2\zeta}\rangle \\ &\quad -\frac{2}{t_{\rm cav}}\langle \Sigma\rangle + \frac{1}{t_{\rm cav}}\langle N\rangle ,\end{aligned} \tag{2.13}$$

where $\Delta N = N - \langle N\rangle$ and

$$\alpha_N(p) = \beta_{N+\zeta}\left[1+\frac{p}{2}(\beta_{N+\zeta}-\beta_{N+2\zeta})\right] . \tag{2.14}$$

The steady-state solution is

$$\begin{aligned}\langle N\rangle &= \zeta N_{\rm ex}\langle \alpha_N\rangle ,\\ \langle \Sigma\rangle &= \frac{1+\zeta}{2}\langle N\rangle + \zeta N_{\rm ex}\langle \Delta\alpha_N \Delta N\rangle \\ &\quad -\frac{pN_{\rm ex}}{2}\zeta^2\langle \beta_{N+\zeta}\beta_{N+2\zeta}\rangle ,\end{aligned} \tag{2.15}$$

where $\Delta\alpha_N = \alpha_N - \langle \alpha_N\rangle$ and $N_{\rm ex} = rt_{\rm cav}$.

We proceed now to an approximate evaluation of the steady-state mean photon number and variance, following the procedure of Ref. [7]. If the population distribution has a peak at some value $\bar{N}$ we may expand

$$\begin{aligned}\beta_{N+\zeta} &= \beta_{\bar{N}+\zeta} + \left.\frac{\partial\beta_{N+\zeta}}{\partial N}\right|_{\bar{N}}(N-\bar{N}) ,\\ \beta_{N+2\zeta} &= \beta_{\bar{N}+\zeta} + \left.\frac{\partial\beta_{N+\zeta}}{\partial N}\right|_{\bar{N}}(N+\zeta-\bar{N}) .\end{aligned} \tag{2.16}$$

The derivatives of the gain coefficients β will be proportional to $\theta_{\rm int}/\sqrt{N_{\rm ex}N}$ for the one-photon micromaser and to $\varphi_{\rm int}/N_{\rm ex}$ for the two-photon micromaser, where $\theta_{\rm int}$ and $\varphi_{\rm int}$ are scaled time variables defined by

$$\begin{aligned}\theta_{\rm int} &= \sqrt{N_{\rm ex}}\,\Omega_{ab}t_{\rm int} ,\\ \varphi_{\rm int} &= 2N_{\rm ex}\frac{\Omega_{ac}^2}{\Delta}t_{\rm int} .\end{aligned} \tag{2.17}$$

Therefore, up to first order in $\theta_{\rm int}/\sqrt{N_{\rm ex}N}$ (for the one-photon micromaser) and in $\varphi_{\rm int}/N_{\rm ex}$ (for the two-photon micromaser) we have

$$\begin{aligned}\langle N\rangle &= \zeta N_{\rm ex}\alpha_{\bar{N}}(0) ,\\ \langle \Sigma\rangle &= \frac{1}{1-\beta'_{\bar{N}+\zeta}}\left[\frac{1+\zeta}{2}\langle N\rangle - \frac{p}{2}\frac{\langle N\rangle^2}{N_{\rm ex}}\right] ,\end{aligned} \tag{2.18}$$

where

$$\beta'_{\bar{N}+\zeta} = \zeta N_{\rm ex}\left.\frac{\partial\beta_{N+\zeta}}{\partial N}\right|_{\bar{N}} . \tag{2.19}$$

For $\zeta=1$, Eq. (2.18) reduces to the expression found in Ref. [7], while for $\zeta=2$ we get a result similar to the one found in Ref. [9]. In terms of the normalized mean photon number $n = \langle N\rangle/(\zeta N_{\rm ex})$ and the normalized variance $\sigma = \langle \Sigma\rangle/\langle N\rangle$, we have then, for the regular (subscript R) and Poissonian (subscript P) pumping cases:

$$\begin{aligned}n_R &= n_P = \alpha_N(0) ,\\ \sigma_R &= \frac{1}{1-\beta'_{\bar{N}+\zeta}}\left[\frac{1+\zeta}{2} - \frac{\zeta}{2}n_R\right] ,\\ \sigma_P &= \frac{1}{1-\beta'_{\bar{N}+\zeta}}\frac{1+\zeta}{2} .\end{aligned} \tag{2.20}$$

Therefore, in this approximation, the mean photon number does not depend on the pumping statistics, while for the variances we have

$$\frac{\sigma_R}{\sigma_P} = 1 - \frac{\zeta}{1+\zeta}n_R . \tag{2.21}$$

The largest noise reduction will occur if $n_R=1$ and therefore it is limited to $\frac{1}{2}$ ($\frac{2}{3}$) for one- (two-) photon masers.

The above expressions should be modified when applied to a laser, in order to take into account the finite atomic lifetime in this case. The gain coefficients should then be averaged over the probability that the atoms have not spontaneously decayed from the lasing levels. Assuming that both levels have the same lifetime, and that the laser is well above threshold, so that the atomic lifetime is small compared to the average Rabi frequency, all gain coefficients β will be averaged to $\frac{1}{2}$. In this situation, we have

$$\begin{aligned}&n_R = n_P = \tfrac{1}{2} ;\\ &\sigma_P = 1 ;\ \ \sigma_R = 0.75 \ \text{(for the one-photon laser)} ;\\ &\sigma_P = 1.5 ;\ \ \sigma_R = 1 \ \text{(for the two-photon-laser)} .\end{aligned} \tag{2.22}$$

It is interesting to remark that for the two-photon micromaser there are values of the interaction time such that the gain coefficient is practically constant, independent of the photon number N. Thus for $\varphi_{\rm int} = 2N_{\rm ex}\pi$ the Rabi angle is always an integer multiple of π and the atoms leave the cavity with the highest probability (almost one for $N>1$) of being deexcited (a "opaque cavity"), the gain coefficient being in this case

$$\beta_{N+\zeta} = \frac{4(N+2)(N+1)}{(2N+3)^2} , \tag{2.23}$$

which is indeed ≈ 1 for large N (already for $N=1$ it is equal to $\frac{24}{25}$). This means that the value of $\langle N\rangle$ builds up in this case to a value close to $2N_{\rm ex}$ ($n\approx 1$), its highest possible value (each atom leaving then two photons in the cavity). The corresponding values of σ_R and σ_P may be easily calculated from Eq. (2.15):

$$\begin{aligned}&n_R = n_P = 1 ,\\ &\sigma_P = 1.5 ,\ \ \sigma_R = 0.5 ,\end{aligned} \tag{2.24}$$

yielding a noise reduction factor $\sigma_R/\sigma_P = 1/3$, the maximum possible reduction allowed by the approximate formula (2.21).

Another peculiar result is obtained when $\varphi_{\rm int}$ is an odd

multiple of $N_{ex}\pi$. In this case the gain coefficient becomes also practically independent of N, and equal to $\frac{1}{2}$ of the value it has in the case of a "opaque cavity": the atom has then a probability $\approx\frac{1}{2}$ of leaving the cavity in its lowest state. In this situation the cavity becomes "semiopaque" or "semitransparent" to the atoms and we obtain the same results for n and σ as for the laser [Eq. (2.22)].

One should be careful however when applying the approximations (2.6) and (2.16) to a micromaser, specially in situations when the number of photons is very small. A similar remark applies to the separate treatment of the gain and loss terms. One expects, however that, if N_{ex} is large enough and if randomness is introduced in the interaction time through a velocity dispersion, the granular character of the system should not play an important role, and Eq. (2.6) should be approximately valid. In fact, as $N\gg1$ and the velocity distribution gets wider, one should recover the results for a laser well above the oscillation threshold, since the gain coefficients also average to $\frac{1}{2}$ in this case.

It is easy to verify explicitly that the limiting results (2.22) hold in this case. The velocity dispersion can be taken into consideration by averaging the gain coefficients with respect to the interaction-time distribution [3,4]. For a Gaussian distribution of interaction times (which corresponds to a Gaussian velocity distribution if the variance $\Delta v \ll \bar{v}$), analytical results are easily obtained:

$$\bar{\beta}_{N+1}=\tfrac{1}{2}\{1-e^{-2\Delta\theta_{\rm int}^2(N+1)/N_{ex}}\times\cos[2\bar{\theta}_{\rm int}\sqrt{(N+1)/N_{ex}}]\} \quad (2.25)$$

for the one-photon micromaser and

$$\bar{\beta}_{N+2}=\frac{2(N+2)(N+1)}{(2N+3)^2}\times\{1-e^{-2\Delta\varphi_{\rm int}^2[(2N+3)/(4N_{ex})]^2}\times\cos[\bar{\varphi}_{\rm int}(2N+3)/(2N_{ex})]\} \quad (2.26)$$

for the two-photon micromaser.

In Eqs. (2.25) and (2.26) $\Delta\theta_{\rm int}$ and $\Delta\varphi_{\rm int}$ stand for the variances of $\theta_{\rm int}$ and $\varphi_{\rm int}$, respectively. If these two quantities become much larger than one, it is easy to see that the corresponding gain coefficients will have a value $\approx\frac{1}{2}$, and we get then the same results for n_R, n_P, σ_R, and σ_P as obtained for the laser [Eq. (2.22)].

We turn now to a detailed consideration of the approximation involved in the separate treatment of the gain and loss terms. This would be justifiable under two conditions: (i) this separation should be possible for the interaction of each individual atom with the cavity field, that is, during the interaction time $t_{\rm int}$; (ii) when considering the field density operator, after the passage of K atoms,

$$\rho(t)=e^{L\Delta t_{K-1}}M(\tau)e^{L\Delta t_{K-2}}M(\tau)\cdots e^{L\Delta t_1}M(\tau)\rho(0)\ , \quad (2.27)$$

where Δt_i is the time interval between atoms $(i+1)$ and i, one should be able to commute the exponential factors through the operators $M(\tau)$.

Condition (i) should hold only if the commutator of $Lt_{\rm int}$ with M is negligible. On the other hand, condition (ii) requires that the commutator or $Lt_{\rm at}$ with M be negligible (considering $t_{\rm at}$ as a typical value of Δt_i). This last condition is more stringent than the first one, since $t_{\rm int}<t_{\rm at}$ for micromasers.

We show now that, for a sufficiently large atomic flux, these commutators may indeed be neglected. As L and M couple only populations among themselves, we can restrict ourselves to the diagonal elements of the commutator,

$$([t_{\rm at}L,M]\rho)_{N,N}=\frac{1}{N_{ex}}\{(N+1)(\beta_{N-\zeta}-\beta_{N+1-\zeta})\pi_{N+1}-\zeta\beta_{N-\zeta}\pi_{N-\zeta}+[(N+1)\beta_{N+1-\zeta}-(N+1-\zeta)\beta_{N-\zeta}]\pi_{N+1-\zeta}\}\ . \quad (2.28)$$

If $N\gg1$ we may expand Eq. (2.28) in powers of $1/N$. If the initial state of the field is the vacuum, values of N much larger than N_{ex} will never contribute to the above expression, and it is then easy to show that the right-hand side of Eq. (2.28) is at most of the order of $\theta_{\rm int}/N_{ex}$ ($\varphi_{\rm int}/N_{ex}$) in the one-photon (two-photon) micromaser case. So long as these quantities remain small, condition (ii), and consequently also condition (i), are satisfied, and the independent treatment of gain and losses is then justified.

If randomness is introduced in the interaction time, as a velocity dispersion, for example, the gain coefficients β approach the value $\frac{1}{2}$ as the velocity spread increases (the same will be true for the laser highly above threshold). In this case, even for small values of N, the corresponding commutator will be of the order of $1/N_{ex}$, so it may be safely neglected for $N_{ex}\gg1$. The same result holds for the "opaque" and "semiopaque" cases discussed in Sec. II for the two-photon micromaser, since the gain coefficients are also independent of N in those situations.

As mentioned above, in order to fulfill just condition (i), milder requirements are necessary, since the relevant commutator in this case, $[t_{\rm int}L,M]\rho$, is obtained by multiplying the above one [Eq. (2.28)] by the factor $t_{\rm int}/t_{\rm at}$, which is always smaller than one in micromasers. This will be the situation in the microscopic approach,

presented in the next section, where the independence between gain and losses will be assumed only during the interaction of each atom with the cavity field.

III. THE MICROSCOPIC APPROACH

The master equation (2.6) should be valid as long as $|p(M-1)| \ll 1$. For the Poissonian case this condition is trivially satisfied, while for regular pumping ($p=1$) it means that the change of the field due to the passage of a single atom is small. This may be not the case in micromasers, where the field intensity may be very weak. Furthermore, in this case the approximations used in Sec. II for getting the values of $\langle N \rangle$ and $\langle \Sigma \rangle$ may not be valid anymore, since they are based on the hypothesis that the steady state is described by a peaked distribution corresponding to a large average photon number. In this sense, we may say that we have developed in Sec. II a *mesoscopic* treatment.

We turn now to a different approach, truly microscopic, which may be applied to study the statistics of the field for micromasers in very weak field situations, down to zero photons inside the cavity. Our aim is to analyze the behavior of both the average photon number and the variance as the pumping statistics is changed from regular to Poissonian. In this process, we will be able to assess the validity of the mesoscopic treatment.

Taking into consideration the losses, the change in the reduced density operator for the field due to the passage of the ith atom is given by [3,4]

$$\rho(t_{i+1}) = e^{L\Delta t_i} M \rho(t_i) , \tag{3.1}$$

where $\Delta t_i = t_{i+1} - t_i$ and L is given by Eq. (2.10).

In writing Eq. (3.1) we assume that the damping time $t_{\rm cav} = Q/\omega$ of the radiation in the cavity is much larger than the interaction time $t_{\rm int}$ of each atom with the cavity field, and treat again the dissipation process as independent of the field-atom interaction (according to the discussion at the end of Sec. II, the precise condition for this to be possible is less strict in the microscopic treatment than in the mesoscopic one, specially if $t_{\rm int} \ll t_{\rm at}$). Otherwise, the present approach differs from the one presented in the previous section by the fact that we do not make any continuous approximation. Instead, we calculate directly from Eq. (3.1), thus finding in a stepwise way the field populations at any instant of time.

Starting from Eq. (3.1), we derive now expressions for the steady-state populations for both the Poissonian and the regular pumping case.

A. Poissonian pumping

If the injected atoms are excited according to a Poissonian statistics, with an average rate r, the distribution of time intervals Δt_i between successive atoms is given by $r \exp(-r\Delta t_i)$. The statistical average of Eq. (3.1) over this distribution yields the change in the mean field density operator [3,4],

$$\bar{\rho}(t_{i+1}) = (1 - L/r)^{-1} M \bar{\rho}(t_i) , \tag{3.2}$$

from which we get the following relation for the photon populations:

$$\pi_N(t_{i+1}) = (1-\beta_{N+\zeta})\pi_N(t_i) + \beta_N \pi_{N-\zeta}(t_i) + \frac{1}{N_{\rm ex}}[(N+1)\pi_{N+1}(t_{i+1}) - N\pi_N(t_{i+1})] , \tag{3.3}$$

where $N_{\rm ex} = r t_{\rm cav}$ and we have suppressed the overbar to simplify the notation.

The set of Eqs. (3.3) allows the calculation of the time evolution of the populations step by step. In the limit of large r (small average time intervals between two consecutive atoms), Eqs. (2.12) and (3.3) are equivalent. For the steady state we have

$$\beta_{N+\zeta}\pi_N - \frac{N+1}{N_{\rm ex}}\pi_{N+1} = \beta_N \pi_{N-\zeta} - \frac{N}{N_{\rm ex}}\pi_N . \tag{3.4}$$

For the one-photon micromaser these relations yield directly an explicit expression for the N-photon population [3]:

$$\pi_N = \frac{N_{\rm ex}^N}{N!}\pi_0 \prod_{j=1}^{(N-1)} \beta_j . \tag{3.5}$$

One may notice from this expression that if for some $N = N_0$ we have $\beta_{N_0} = 0$ (which corresponds to an integer number of turns of the atomic Bloch vector, as the atom crosses the cavity), then all higher-N populations will vanish. One says then that $N = N_0$ corresponds to a *trapping state* [12]. In the limit of negligible damping ($Q \to \infty$), the photon population will concentrate on these values of N, giving rise to Fock states. For zero damping, these solutions are however only marginally stable (stable from the left and unstable from the right), each trapping state attracting all the population between itself and its nearest left neighbor. For finite damping, trapping states leave still their signature, being transformed into the extrema of the population distribution. For very low damping, and as the interaction time between the atom and the cavity field is modified (by changing, for instance, the atomic speed), that distribution may display very sharp peaks (reminiscent of the zero-dissipation Fock states),sometimes associated with very low populations. In this case, the average number of photons decreases abruptly, so the corresponding curve as a function of $t_{\rm int}$ displays sharp holes, at precisely the same points where the variance becomes very small [12].

For the two-photon micromaser ($\zeta = 2$), we may use directly the recursion relation (3.4) to get numerically the steady-state population. Explicit expressions in terms of continued fractions may also be found [13]. A detailed discussion of the dynamical effects of trapping states for one- and two-photon micromasers has been presented in Ref.[14].

B. Regular pumping

To find the population change in the case that the incoming atoms arrive in the cavity at a regular rate $r = 1/t_{\rm at}$, we first diagonalize the superoperator L. The

action of L on a density operator in the photon-number representation is given by

$$[t_{at}L\rho]_{N,N+l}=\mathcal{L}(l)_N^{N'}\rho(l)_{N'}\ , \tag{3.6}$$

where we used the convention that repeated indices are summed, $\rho(l)_N\equiv\rho_{N,N+l}$ and

$$\mathcal{L}(l)_N^{N'}\equiv(1/N_{ex})[\sqrt{N'(N'+l)}\delta_{N+1}^{N'}-(N+l/2)\delta_N^{N'}]\ . \tag{3.7}$$

For each l we can find the right, $|v_k\rangle$, and left, $\langle w_k|$, eigenvectors of the operator $\mathcal{L}(l)$, belonging to the eigenvalues

$$\lambda_k=-(k+l/2)/N_{ex}\ . \tag{3.8}$$

The components of these eigenvectors in the photon-number basis are given by

$$\langle N|v_k\rangle=\begin{cases}(-1)^N\dfrac{k!}{(k-N)!}\left[\dfrac{l!}{N!(N+l)!}\right]^{1/2}, & N\le k\\ 0\ , & N>k\ ,\end{cases} \tag{3.9}$$

$$\langle w_k|N\rangle=\begin{cases}(-1)^k\dfrac{1}{k!(N-k)!}\left[\dfrac{N!(N+l)!}{l!}\right]^{1/2}, & N\ge k\\ 0\ , & N<k\ .\end{cases}$$

The right and left eigenvectors defined above have been normalized so that $\langle w_k|v_{k'}\rangle=\delta_k^{k'}$, and satisfy the closure relation.

Using Eqs. (3.7)–(3.9), we can easily find the change in population after the passage of one atom:

$$\pi_N(t+t_{at})=e^{-\delta N}\sum_{j=0}^{\infty}\frac{(N+j)!}{N!j!}(1-e^{-\delta})^j\Gamma_{j+N}(t)\ , \tag{3.10}$$

where

$$\Gamma_N=(1-\beta_{N+\zeta})\pi_N+\beta_N\pi_{N-\zeta}\ , \tag{3.11}$$

and $\delta=1/N_{ex}$. The steady-state populations satisfy Eq. (3.10) with the left-hand side replaced by π_N (independent of t). The resulting expression is quite different in form from the one obtained for Poissonian pumping. In fact, it couples the $(N-\zeta)$ population to all higher-N populations. In order to use this expression for numerical calculations, in the case of one-photon micromasers, we set $\pi_{N_0}=0$ for some sufficiently large N_0, and calculate the lower-N populations starting from an arbitrary value for π_{N_0-1}, which is later found out by means of the normalization condition. This approach is actually quite natural for one-photon micromasers, when a trapping state is found for some $N=N_0$, since the populations then vanish for $N>N_0$. These trapping states correspond, also in the regular-pumping case, to the zeros of the gain function β_N. Indeed, one sees from (3.10) and (3.11) that the populations π_N, $N>N_0-\zeta$, get decoupled from the lower-N populations, if $\beta_{N_0}=0$.

For the two-photon micromaser, this approach does not work since after setting $\pi_{N_0}=0$ one would need to specify the values of both π_{N_0-1} and π_{N_0-2}, in order to be able to calculate all lower-N populations.

We adopted therefore an alternative method for finding numerically the steady state in this case: we used the dynamical relation (3.10) to calculate the time evolution of the populations, starting from the vacuum state, and checking for the attainment of the asymptotic values. This procedure was applied also to the one-photon micromaser, and compared to the calculation based on the steady-state equation, thus allowing us to check that both methods lead to the same results in this case.

IV. NUMERICAL RESULTS

We present now the results of the numerical calculations based on the formalism developed in Sec. III, and compare them to those obtained from the p-dependent master equation (2.11). Our results will be presented as functions of the reduced interaction times, θ_{int} for the one-photon micromaser and φ_{int} for the two-photon micromaser, as defined in Sec. II, Eq. (2.17). We expect that large differences between the behavior of masers and micromasers should appear for small values of N_{ex} and for interaction times such that the field statistics may be dominated by a low-N trapping state [12,14] (or, equivalently, by a low-N peak in the photon-number distribution), so that N is much smaller than the greatest possible value of the mean photon number, given by ζN_{ex} (each atom releases then ζ photons in the cavity).

According to the discussion in the previous section, for low dissipation this will happen whenever the atomic Bloch vector makes an integer number q of turns as the atom crosses the cavity:

$$\theta_{int}\frac{\sqrt{N_q+1}}{\sqrt{N_{ex}}}=\pi q \tag{4.1}$$

for the one-photon micromaser and

$$\varphi_{int}\frac{2N_q+3}{4N_{ex}}=\pi q \tag{4.2}$$

for the two-photon micromaser, with N_q of the order of one. These equations allow therefore an easy estimate of the approximate positions of the maxima of the photon-number distribution (for zero dissipation, they allow the precise determination of the trapping states).

We first present the results for the one- and two-photon micromasers within the formalism of Sec. III. Next we compare these results with those obtained from the master equation (2.11).

A. One-photon micromaser

In Fig. 1 we display the results for the steady-state normalized mean photon number $n=\langle N\rangle/N_{ex}$ for regular (n_R) and Poissonian (n_P) pumping, in the case that $N_{ex}=49$ and for a monokinetic beam. This particular choice of N_{ex} was made in order to render immediate the (approximate) identification of the photon-number distri-

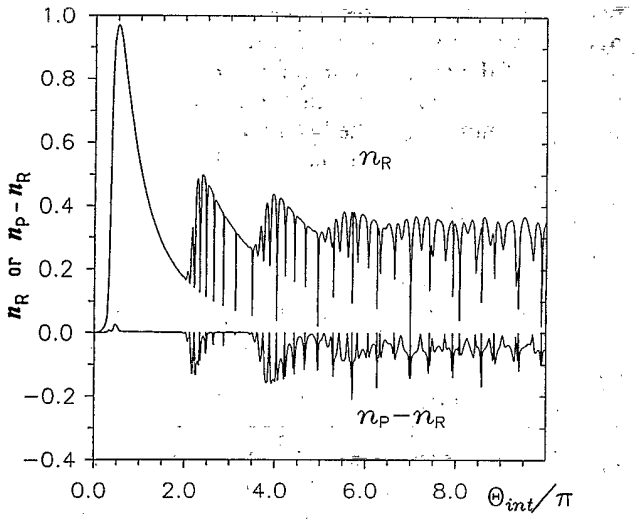

FIG. 1. One-photon micromaser. Normalized mean photon number n_R for regular injection and the difference $n_P - n_R$ between the normalized photon numbers for regular and Poissonian statistics at steady state, as functions of the reduced interaction time θ_{int}. $N_{\text{ex}}=49$ and $\Delta v=0.0$ (monokinetic atomic beam).

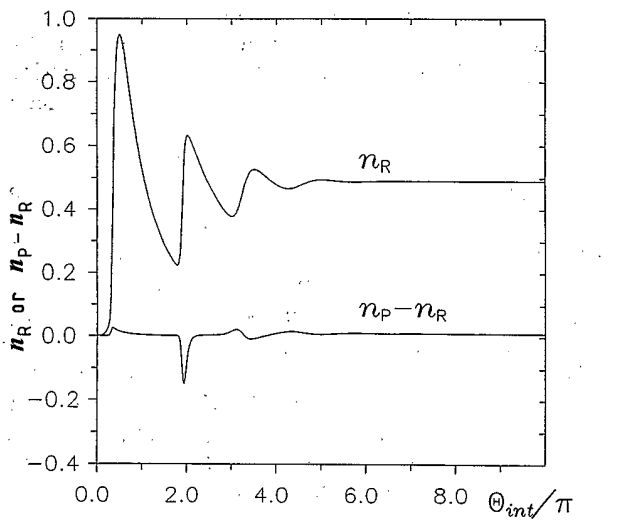

FIG. 2. One-photon micromaser. Same as Fig. 1 for a velocity dispersion $\Delta v=0.1\bar{v}$.

bution peaks [cf. Eq. (4.1)].

The singular behavior of the field as a function of the interaction time is quite apparent. Both n_R and n_P suffer abrupt changes around values of the interaction time for which new dominating peaks show up in the photon-number distribution. Furthermore, when these peaks occur for low values of N ($N \ll N_{\text{ex}}$), the difference between n_R and n_P becomes very large. Except for a small region around the oscillation threshold, n_R is usually larger than n_P. Large differences occur throughout the whole studied interval of θ_{int}, as can be seen in Fig. 1. This variation in the average photon number is associated with the p dependence of the gain coefficient, explicitly displayed in Eq. (2.14), and which cannot be neglected in this case, due to the low values of N.

We expect that these differences should disappear when we introduce randomness in the system. In Fig. 2 we show the same variables in the case that the beam has a Gaussian velocity distribution with a variance Δv equal to 10% of the mean velocity $\bar{v}$. We see that the large differences between n_R and n_P do not disappear near $\theta_{\text{int}}=2\pi$, where they correspond to about $\frac{1}{4}$ of n_P, while for most other values of θ_{int} the difference becomes very small, in agreement with Eq. (2.20).

In Fig. 3 we display, for a monokinetic beam, the steady-state value of the normalized variance $\sigma=\Sigma/\langle N\rangle$ for regular pumping, σ_R, and the ratio of the steady-state normalized variances for regular and Poissonian pumping (σ_R/σ_P). We notice again an extremely singular behavior. The quick alternance between sub-Poissonian and super-Poissonian statistics is a consequence of the fact that the field is successively dominated by only one or more population peaks. Figure 3(b) makes it clear that regularization of the pumping may result not only in large noise reduction (as much as $\approx 85\%$), much beyond that predicted by the mesoscopic treatment [Eq. (2.21)], but also in noise amplification. This happens because the very shape of the distribution is affected by the pumping statistics: the relative heights of the population peaks depend on the statistical parameter p, so that, for some interaction times, setting $p=1$ (regular pumping) results in the reduction of the dominance of one of those peaks and the consequent increase in the field variance.

The behavior displayed in Fig. 3 is however not very realistic, since it corresponds to a monokinetic beam. In Fig. 4 we display the same variables for a Gaussian velocity distribution with a 10% velocity spread ($\Delta v/\bar{v}=0.1$), which corresponds approximately to a Gaussian distribution of interaction times with the same spread. We see that for small interaction times ($\bar{\theta}_{\text{int}}/\pi<5$) the normalized variances σ_R and σ_P are still very singular, with a general behavior quite different from the one predicted by Eq. (2.20). As before, either noise reduction or amplification may be obtained in this region of $\bar{\theta}_{\text{int}}$, as one goes from Poissonian to regular pumping. Maximum noise reduction is obtained for $\bar{\theta}_{\text{int}}\approx 2\pi$, where $\sigma_R/\sigma_P\approx 1/4$. For large interaction times ($\bar{\theta}_{\text{int}}/\pi>6$), the variances behave as predicted in Sec. II for a laser well above threshold [Eq. (2.22)], since for large $\bar{\theta}_{\text{int}}$ the gain coefficient β approaches $\frac{1}{2}$ [cf. Eq. (2.25)]: we get then the usual Poissonian result for Poissonian pumping, and a noise reduction of 25% for regular pumping.

From these results we see that the regularization of the pumping preserves the singular behavior of the average photon number, which was studied in Ref. [12] for a Poissonian pumping.

B. Two-photon micromaser

As opposed to the one-photon device, the two-photon degenerate micromaser displays a remarkable symmetry with respect to the interaction time: the gain coefficients $\beta_{N+\xi}$ are periodic functions of the normalized interaction time φ_{int}, with period $4\pi N_{\text{ex}}$. Furthermore, they are sym-

metric with respect to $2\pi N_{ex}$. The scaled variables n and σ will therefore exhibit the same symmetries, and this is clearly displayed in Figs. 5 and 6 (our calculations for the two-photon micromaser have been made for $N_{ex}=15$).

In Fig. 5 we display the steady-state results for n_R and n_P. From Eq. (2.20), we expect $n_R \approx n_P$. This is not true in general as we can see in Fig. 5(b). As we increase the interaction time and therefore φ_{int}, the average photon number for regular pumping, n_R, starts to build up before the average photon number for Poissonian pumping, n_P. This means that the oscillation threshold is lowered as the pumping is regularized. This effect is related to the first-order phase transition behavior of the two-photon micromaser: at threshold, the population distribution has two peaks of equal heights, one of them at $N=0$. The exact value of φ_{int} for which this situation is attained is however sensitive to the pumping statistics. For the one-photon micromaser, a second-order phase transition analogy holds for the oscillation threshold, and the gradual increase of the average photon number as one goes above threshold turns out to be much less sensitive to the statistics of the pumping. The behavior of n_R and n_P close to threshold for the two-photon micromaser is clearly shown in the inset of Fig. 5(b): the threshold value of φ_{int} for regular pumping is in this case about 20% below the value corresponding to Poissonian pumping. This may be probably the easiest experimental check of our model.

The sharp decrease of the average number of photons at $\varphi_{int}=20\pi$, 40π, and 60π, shown in Fig. 5(a), is associated with the dominance of a population peak around $N=0$, corresponding to the periodic attainment of the bellow-threshold situation. The sharp depressions at $\varphi_{int}\approx 28\pi$ and 32π are associated with the dominance of population peaks around $N\approx 6$ (the population distribution for these values of φ_{int} was studied in Ref. [14]). The

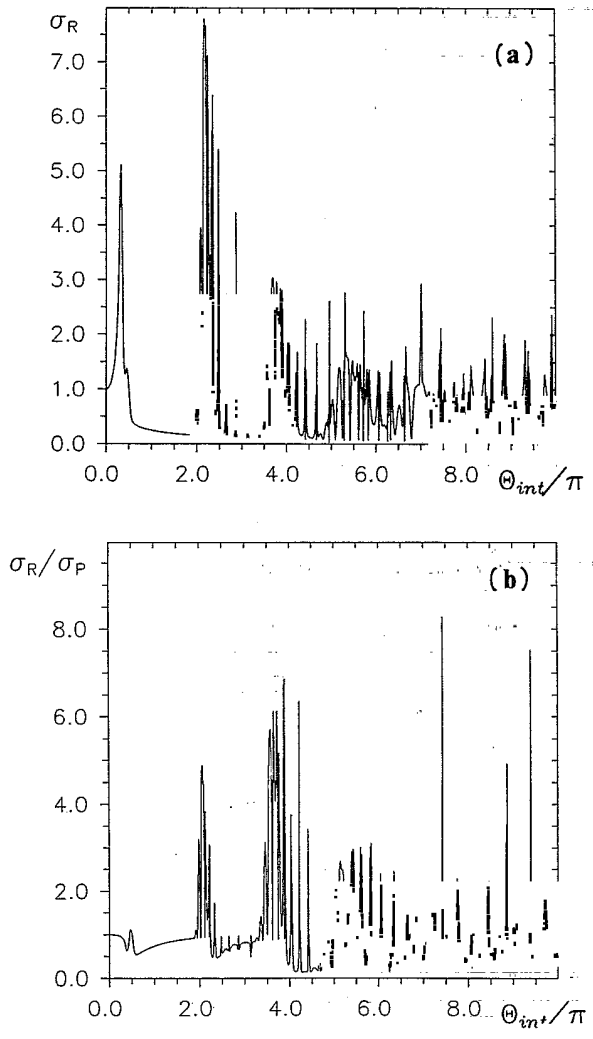

FIG. 3. One-photon micromaser. Steady-state normalized photon-number variances σ_R (regular statistics) and σ_P (Poissonian statistics) as functions of the reduced interaction time θ_{int}: (a) σ_R; (b) σ_R/σ_P. $N_{ex}=49$ and $\Delta v=0.0$.

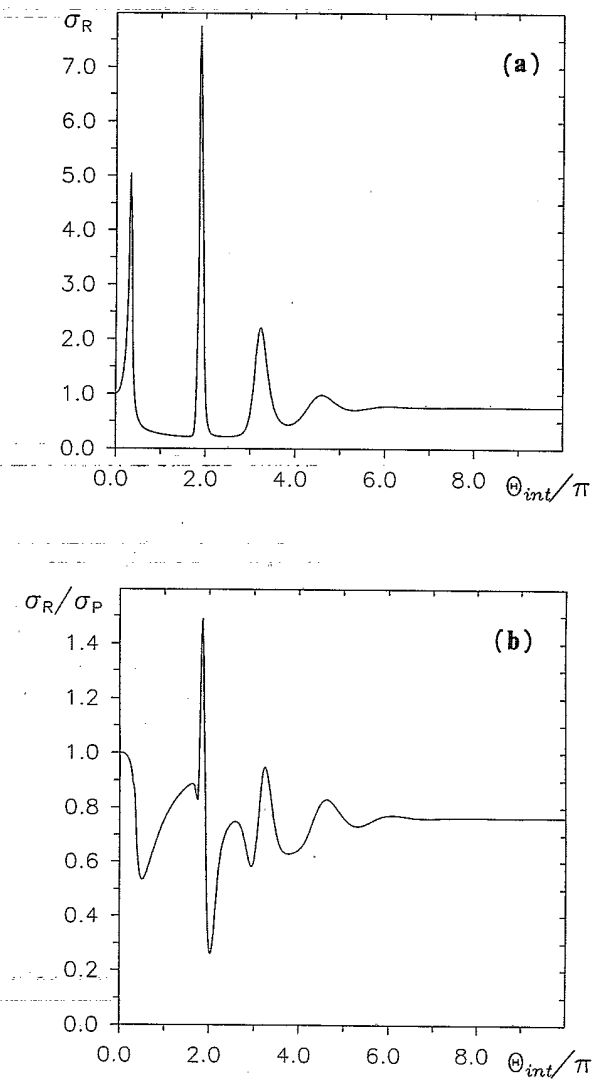

FIG. 4. One-photon micromaser. Same as Fig. 3 for a velocity dispersion $\Delta v=0.1\bar{v}$.

sharp peak at $\varphi_{\rm int}=(2\pi N_{\rm ex})=30\pi$ corresponds to the "opacity" of the cavity [14] discussed in Sec. II: each atom delivers then practically all of its energy to the cavity. We have in this case $n\approx 1$ as predicted.

The "semiopaque" case discussed in Sec. II is also displayed in Fig. 5. For $\varphi_{\rm int}=15\pi$ or 45π (odd multiples of $N_{\rm ex}\pi$), the atom has a probability of $\approx\frac{1}{2}$ of leaving the cavity in its lowest state, and $n\approx\frac{1}{2}$. The overall tendency of the average photon number to increase as the pumping is regularized is also quite clear in this case: even after the threshold for Poissonian pumping, n_R may become up to 50% larger than n_P.

In Fig. 6 we display the results for σ_R and σ_R/σ_P. As in the one-photon case, Eq. (2.20) does not describe correctly the variance in regions where low-N population peaks dominate. In these cases, as the pumping statistics is changed from Poissonian to regular, a noise reduction much larger than that predicted by Eq. (2.21) may occur. Noise reduction is specially effective for a "opaque cavity" ($\varphi_{\rm int}=30\pi$), where $\sigma_R/\sigma_P=1/3$, as predicted by Eq. (2.24), and for the operating points $\varphi_{\rm int}\approx 28\pi$ and 32π, which have been already singled out in the above discussion. For these two points, we get a large noise reduction, with $\sigma_R/\sigma_P\approx 0.24$. Very large noise reduction also occurs near the semiclassical threshold, as can be seen in the inset of Fig. 6(b), where σ_R/σ_P reaches a low value of ≈ 0.11 at $\varphi_{\rm int}\approx 0.59$, and at the corresponding symmetrical region near $\varphi_{\rm int}=4\pi N_{\rm ex}$. This large noise reduction is related to the dependence of the threshold on the pumping statistics, as discussed before. Noise amplification also occurs for the two-photon micromaser,

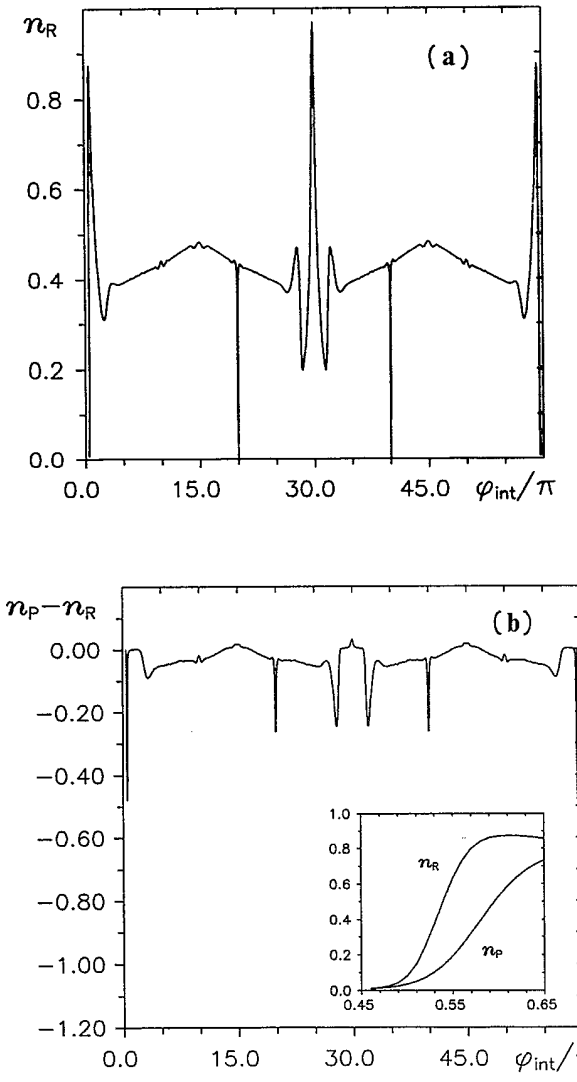

FIG. 5. Two-photon micromaser. Steady-state normalized mean photon numbers n_R (regular statistics) and n_P (Poissonian statistics) as functions of the reduced interaction time $\varphi_{\rm int}$: (a) n_R; (b) n_P-n_R. In the inset we show the behavior of n_R and n_P near the oscillation threshold. $N_{\rm ex}=15$ and $\Delta v=0.0$.

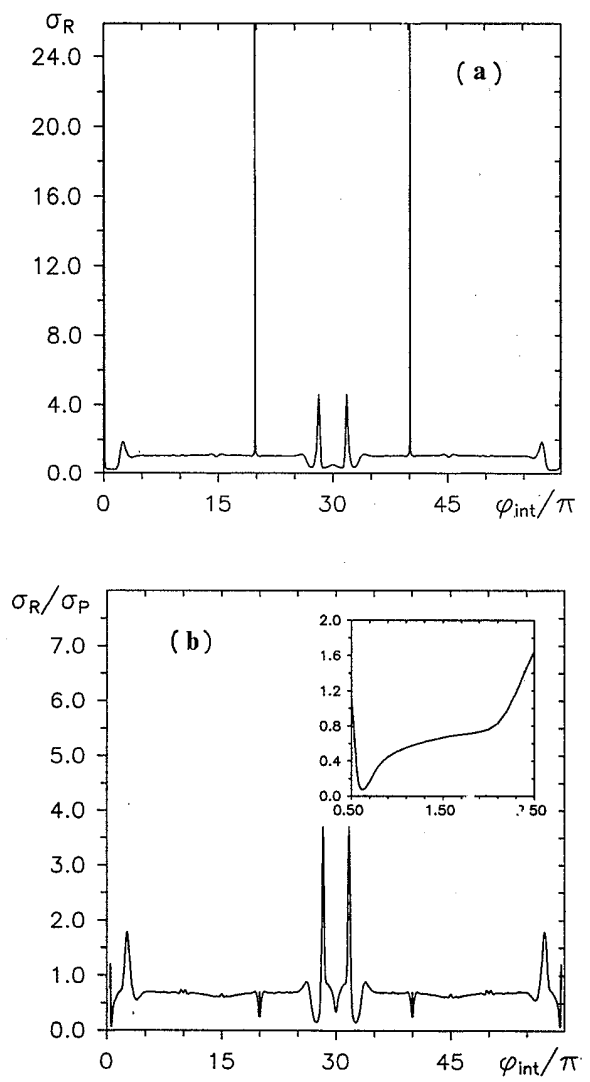

FIG. 6. Two-photon micromaser. Steady-state normalized photon-number variances σ_R (regular statistics) and σ_P (Poissonian statistics) as functions of the reduced interaction time $\varphi_{\rm int}$: (a) σ_R; (b) σ_R/σ_P. In the inset we show the behavior near the oscillation threshold. $N_{\rm ex}=15$ and $\Delta v=0.0$.

as shown in Fig. 6, and it is due, as in the one-photon micromaser case, to the p dependence of the relative heights of the population peaks.

We consider now that the atomic beam has a Gaussian velocity distribution, with a 10% spread as before. The results for n and σ are displayed in Figs. 7 and 8, differing appreciably from the approximate expression (2.20) only in the region where φ_{int} is small. We notice that it is still true that n_R starts to build up before n_P. Very large noise reduction occurs as before near the semiclassical threshold, reaching the value $\sigma_R/\sigma_P \approx 0.09$ at $\varphi_{\text{int}} \approx 0.63$. For $\varphi_{\text{int}} > 1.5\pi$, maximum noise reduction is obtained for $\varphi_{\text{int}} \approx 3.5\pi$, where $\sigma_R/\sigma_P \approx 0.56$. For larger values of φ_{int}, we get $\sigma_R/\sigma_P \approx 2/3$ and $n \approx \frac{1}{2}$, as predicted by Eq. (2.22).

C. Comparison with the p expansion

As expected, the master equation (2.11) is not able to reproduce the results obtained from the microscopic equations of Sec. III, specially if the atomic beam is monokinetic and low-N population peaks become important. We have compared the results obtained numerically from the p expansion [Eq. (2.11)] with those discussed before (corresponding to the microscopic approach), both for the one-photon and the two-photon micromaser. For a monokinetic beam we found that the disagreement is very large in the whole region of θ_{int} (φ_{int}), specially in regions where low-N population peaks dominate. The discrepancy between the two approaches remains important even when a velocity dispersion of the order of 10% is allowed.

In Figs. 9 and 10 we show, for velocity dispersions of 0.5% ($\Delta v/\bar{v} = 0.005$) and 10% ($\Delta v/\bar{v} = 0.10$), the relative differences R_n and R_σ between the results for the mean photon number and the normalized variance, respectively, as obtained from the microscopic approach and from the first-order p expansion, normalized to the microscopic results. Discrepancies are larger for small average interaction times, since in this case the absolute dispersion in interaction times is also small (for a given percentual dispersion). For the same reason, the results are quite independent of the percentual dispersion, in the region of small interaction times.

For the one-photon micromaser, as it is shown in Fig. 9(a) [Fig. 10(a)], the discrepancies are very large for a velocity dispersion of 0.5% and may reach values that are larger than 40% (300%) for the mean photon number (normalized variance). For a dispersion of 10%, R_n and R_σ become much smaller, but R_σ may still reach values as a large as 22%.

For the two-photon micromaser [Figs. 9(b) and 10(b)], the discrepancies in the region of small interaction times

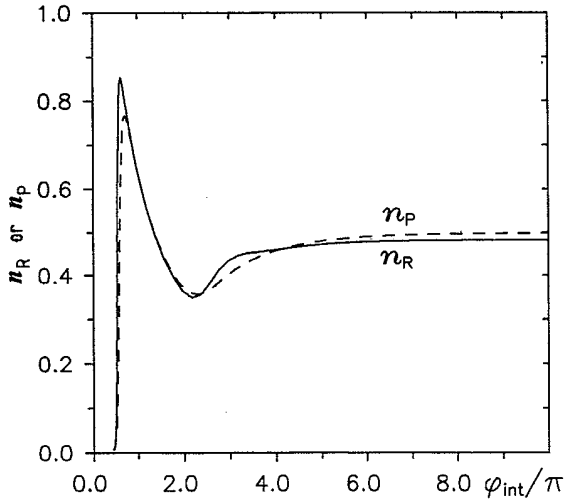

FIG. 7. Two-photon micromaser. Steady-state normalized mean photon numbers n_R (regular statistics) and n_P (Poissonian statistics) as functions of the reduced interaction time φ_{int}. $N_{\text{ex}} = 15$ and $\Delta v = 0.1\bar{v}$.

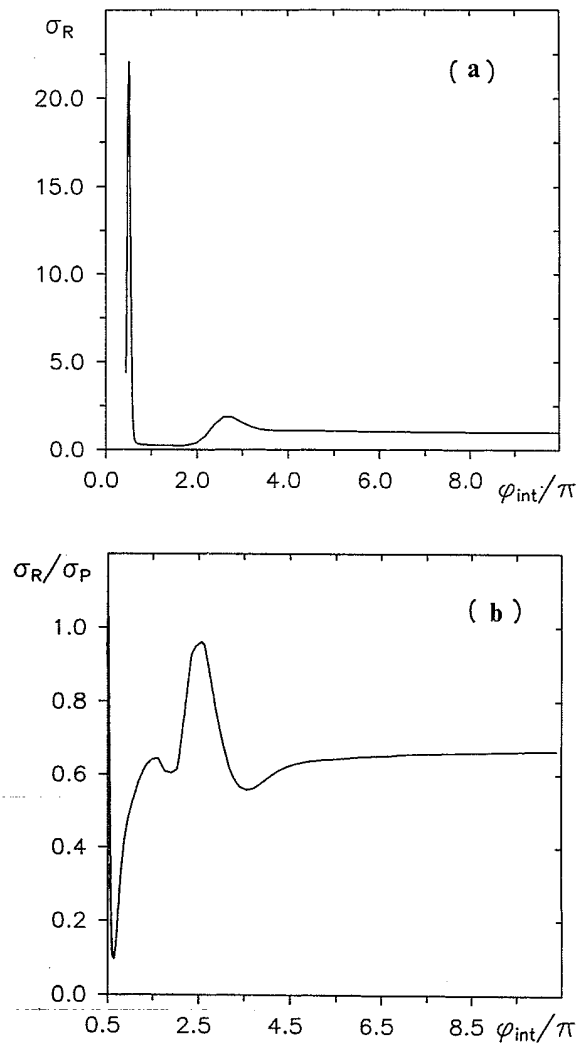

FIG. 8. Two-photon micromaser. Steady-state normalized variances σ_R (regular statistics) and σ_P (Poissonian statistics) as functions of the reduced interaction time φ_{int}: (a) σ_R; (b) σ_R/σ_P. $N_{\text{ex}} = 15$ and $\Delta v = 0.1\bar{v}$.

are still very large for both velocity dispersions, reaching values larger than 30% (200%) in the mean photon number (normalized variance). These high values occur in a region around the oscillation threshold [displayed as an inset in Figs. 9(b) and 10(b)] where the photon distribution is characterized by two peaks of about equal heights and therefore a large variance. This implies a large sensitivity to approximations, since at threshold a small change in the relative heights of the two peaks implies a large change in the variance. Furthermore, just below threshold the average photon number is very small, thus invalidating the use of the first-order p expansion.

Out of this region, the values of R_n are not so large, but R_σ still reach values larger than 50% (25%) for a velocity dispersion of 0.5% (10%). One might think that the large values of R_σ for $\varphi_{\rm int}$ small is a reflection of the large values of R_n. This is not the case: we have checked this possibility by calculating the discrepancies in the variances (not normalized to the photon number) and found them to be also extremely large.

One should also remark that the master equation (2.11), based on an expansion in powers of the statistical parameter p, is not well suited to treat the initial evolution of the micromaser for a regular injection of atoms, since convergence of the expansion in this case is assured only for large photon numbers [4], while very small photon numbers are involved in the beginning of the process.

V. CONCLUSIONS

We have presented a microscopic model to discuss the photon statistics of the one- and two-photon micromaser

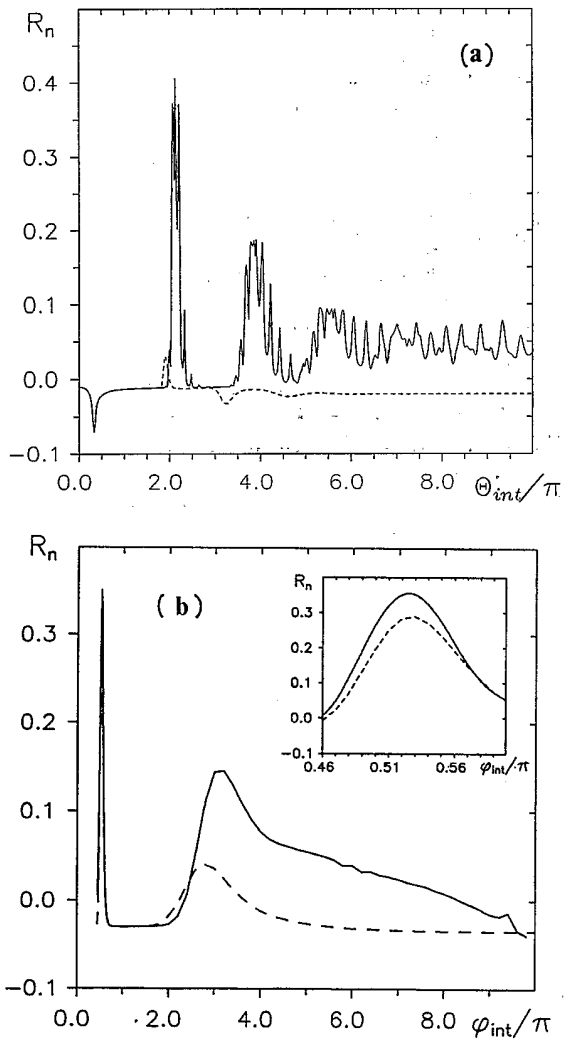

FIG. 9. Regular pumping. Relative difference $R_n = (\bar{N}_m - \bar{N}_p)/\bar{N}_m$ between the steady-state mean photon numbers calculated using the microscopic approach ($\bar{N}_m$) and the first-order p expansion of the master equation ($\bar{N}_p$), as a function of the reduced, interaction time, for $\Delta v = 0.005\bar{v}$ (solid line) and for $\Delta v = 0.10\bar{v}$ (dashed line): (a) one-photon micromaser ($N_{\rm ex} = 49$); (b) two-photon micromaser ($N_{\rm ex} = 15$)—the inset displays the region around the oscillation threshold.

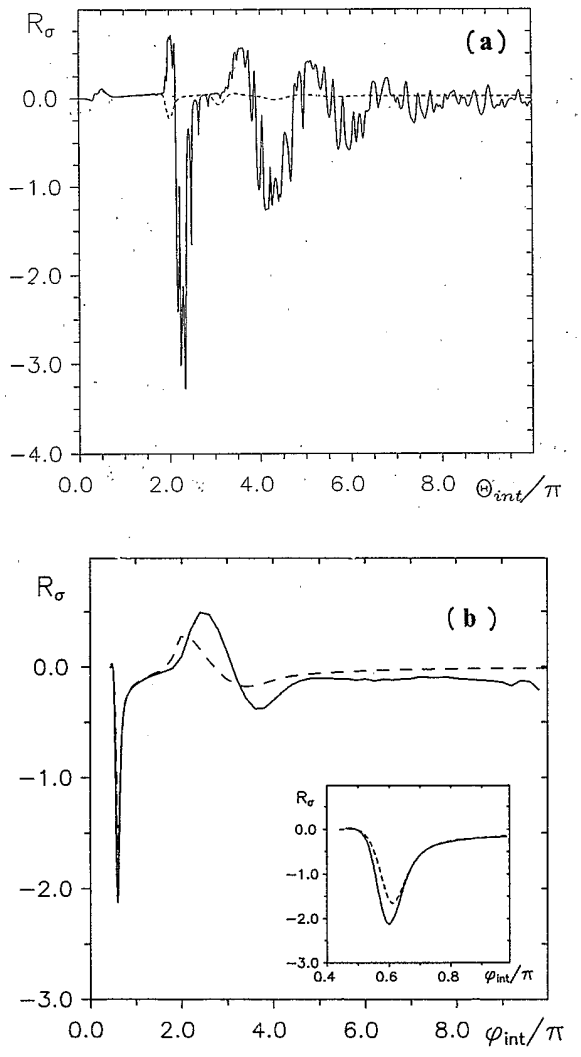

FIG. 10. Regular pumping. Relative difference $R_\sigma = (\sigma_m - \sigma_p)/\sigma_m$ between the steady-state normalized variances calculated from the first-order p expansion of the master equation (σ_p) and the microscopic approach (σ_m), as a function of the reduced interaction time, for $\Delta v = 0.005\bar{v}$ (solid line) and for $\Delta v = 0.005\bar{v}$ (dashed line): (a) one-photon micromaser ($N_{\rm ex} = 49$); (b) two-photon micromaser ($N_{\rm ex} = 15$)—the inset displays the region around the oscillation threshold.

with regular atomic injection, and have shown that the variance of the field may be substantially decreased, with respect to the Poissonian case, much more than for macroscopic lasers and masers. This means that the highly singular behavior of micromasers at low temperatures, reminiscent of the zero-dissipation trapping states [12,14] is greatly enhanced when the excited atomic beam is injected in a regular way. Even though this effect is much more important for monokinetic beams, large noise reduction may still occur even in the presence of a velocity spread of about 10%. Another important result concerns the behavior of the average photon number near the semiclassical threshold, for the two-photon micromaser: regularization of the pumping leads to lower values of the oscillation threshold.

Our results make also clear that care must be taken when applying a master equation approach to the regular-pumped micromaser. For monokinetic beams, and in situations where small photon numbers are involved, the microscopic method leads to field variances which are quite different from those obtained via the master equation treatment. Even for a velocity spread of 10%, the discrepancy between the two approaches may attain very large values.

ACKNOWLEDGMENTS

This work was partially supported by CAPES, CNPQ, FAPERJ, and FINEP.

[1] D. Meschede, H. Walther, and G. Müller, Phys. Rev. Lett. **54**, 551 (1985).

[2] M. Brune, J. M. Raimond, P. Goy, L. Davidovich, and S. Haroche, Phys. Rev. Lett. **59**, 1899 (1987).

[3] P. Filipowicz, J. Javanainen, and P. Meystre, Phys. Rev. A **34**, 3077 (1986).

[4] L. Davidovich, J. M. Raimond, M. Brune, and S. Haroche, Phys. Rev. A **36**, 3771 (1987).

[5] G. Rempe, F. Schmidt-Kaler, and H. Walther, Phys. Rev. Lett. **64**, 2783 (1990).

[6] M. Golubev and I. V. Sokolov, Zh. Eksp. Teor. Fiz. **87**, 408 (1984) [Sov. Phys.—JETP **60**, 234 (1984)].

[7] J. Bergou, L. Davidovich, M. Orszag, C. Benkert, M. Hillery, and M. O. Scully, Opt. Commun. **72**, 82 (1989); Phys. Rev. A **40**, 5073 (1989).

[8] Y. Yamamoto, S Machida, and O. Nilsson, Phys. Rev. A **34**, 4025 (1986); T. A. B. Kennedy and D. F. Walls, *ibid.* **40**, 6366 (1989); F. Haake, S. M. Tan, and D. F. Walls, *ibid.* **41**, 2808 (1990).

[9] M. Orszag and J. C. Retamal, Opt. Commun. **79**, 455 (1990).

[10] For weak pumping and weak photon damping the equivalence between the microscopic approach and the master equation was demonstrated, independently of the pumping statistics, by L. Lugiato, M. O. Scully, and H. Walther, Phys. Rev. A **36**, 740 (1987).

[11] M. Sargent III, M. O. Scully, and W. E. Lamb Jr., *Laser Physics* (Addison-Wesley, Reading, MA, 1974).

[12] P. Filipowicz, J. Javainainen, and P. Meystre, J. Opt. Soc. Am. B **14**, 906 (1986); P. Meystre, G. Rempe, and H. Walther, Opt. Lett. B **14**, 1078 (1988).

[13] I. Ashraf, J. Gea-Banacloche, and M. S. Zubairy, Phys. Rev. A **42**, 6704 (1990).

[14] C. R. Carvalho, L. Davidovich, and N. Zagury, Opt. Commun. **72**, 306 (1989).